

pubs.acs.org/JPCC Article

Benzene Adsorbed on Activated Carbon: A Comprehensive Solid-State Nuclear Magnetic Resonance Study of Interactions with the Pore Surface and Molecular Motions

Jordon W. Benzie, Vladimir I. Bakhmutov,* and Janet Blümel*



Cite This: J. Phys. Chem. C 2020, 124, 21532-21537



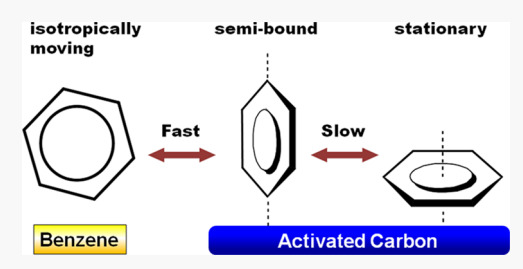
ACCESS I

III Metrics & More



S Supporting Information

ABSTRACT: Benzene- d_6 and cyclohexane- d_{12} have been adsorbed on the surface within the pores of high-surface-area activated carbon (**AC**). Their molecular motions have been characterized by variable-temperature 2 H and 13 C solid-state NMR spectroscopy. Three different states of benzene molecules on the **AC** surface have been found: isotropically moving molecules, bound molecules, and intermediates between these states. In contrast to cyclohexane, benzene assumes stationary states that are stabilized by π -p interactions with the **AC** surface. Hereby, fast in-plane C_6 rotations take place. The adsorption enthalpy $-\Delta H^0$ for benzene on the surface of **AC** within the pores was determined as 4.6 ± 0.3 kcal/



mol. The strongly adsorbed molecules undergo slow exchange with isotropically moving, liquid-like molecules. In contrast to this, exchange between the molecules in a liquid-like state with benzene in semibound states (T-complexes) is very fast, requiring only low activation energies $E_{\rm act}$ and ΔH^{\ddagger} of 3.1 and 2.7 kcal/mol, respectively.

■ INTRODUCTION

Activated carbon (AC), featuring a high surface area and porosity, attracts great attention in diverse fields of chemistry as an inexpensive and indispensable material. AC is of enormous importance for applications in chemistry, medicine, and industry, for example, for gas and water purifications, metal extractions, and many others. ^{1,2} During past decades, diverse carbon materials have been studied by different physicochemical methods, ^{3–18} including NMR spectroscopy, ^{3–5,16–19} thermal analysis, ^{5–7,14,15} X-ray^{10,12} and neutron diffraction, ⁷ and FTIR. ⁵ Additionally, theoretical calculations ^{8,9,11,13} and thermochemical studies of simple organic molecules, adsorbed on AC surfaces from vapors and solutions (benzene, toluene, ethyl chloride, carbon tetrachloride, and many others), have been performed. ^{20–24}

In spite of the many results obtained so far, currently, there is only limited knowledge about the molecular dynamics of adsorbates and their interactions with the surface in AC pores. Even for benzene, only limited information has been reported, although it often serves as a reference molecule in adsorption studies. For example, benzene molecules on nonporous graphitized carbon black have been characterized by low-temperature 2H T_1 relaxation time measurements interpreted by low-energy hexad axis benzene reorientations (fast in-plane C_6 rotations). Similar results have been obtained for ^{13}C -enriched benzene adsorbed on the surface of charcoal when it was probed by ^{13}C solid-state NMR spectroscopy. 27

Recently, ferrocene ((C₅H₅)₂Fe) has been adsorbed on silica and activated carbon surfaces. Although ferrocene is an organometallic compound that obviously differs from benzene,

it features aromatic cyclopentadienyl rings as ligands. Each cyclopentadienyl ring is planar and contains six π electrons, in analogy to benzene. On AC surfaces within the pores, ferrocene showed liquid-like behavior with fast exchange between isotropically moving molecules and surface-attached horizontally oriented ferrocene molecules. The adsorption enthalpy ΔH^0 has been determined to be in the range of -8.4 to -7.0 kcal/mol. In the surface-attached state, the C_5H_5 rings display fast rotation and they are perpendicular to the pore surface. Since the in-plane C_6 rotating benzene molecules are oriented parallel to the surface on nonporous graphitized carbon black 26,27 and perpendicular to a graphite surface, 29 the characteristics of benzene in the pores of AC are of great interest in order to gain a deeper insight into the general factors that determine its surface orientation and dynamics.

Activated carbon (charcoal) consists of nongraphitic carbon with complex surface characteristics and ranges of pore sizes from 2 to >50 nm.² In addition, depending on the manufacturing processes and starting materials, AC can contain different surface groups, impurities, and irregularities.²⁰ Therefore, the precise atomic structure of AC is still unknown.³⁰ In addition, AC is a paramagnetic material and active in electron paramagnetic resonance (EPR),^{31,32} thus

Received: July 7, 2020 Revised: August 27, 2020 Published: September 1, 2020





complicating the application of NMR techniques for probing the adsorbate dynamics of benzene. Although paramagnetic solid-state NMR has successfully been applied, for example, to surface-adsorbed metallocenes^{33,34} and aromatic compounds on a graphitic surface,²⁹ the paramagnetism of **AC** might have deterred chemists from applying this method. Nevertheless, solid-state NMR spectroscopy has been successfully used for studies of the molecular dynamics of ferrocene on the paramagnetic surface of **AC**, as mentioned above.²⁸ Finally, only for small molecules, investigations have been performed using theoretical molecular dynamics simulations to describe, for example, the translational and rotational diffusion of methane molecules in carbon nanotubes.^{35,36}

METHODS

In this contribution, we report the comprehensive solid-state NMR study of a commercial AC (DARCO), ³⁷ containing 370 mg and 620 mg of benzene- d_6 per 1 g of AC (materials AC-C₆D₆-370 and AC-C₆D₆-620, respectively), and 55 mg of cyclohexane- d_{12} (sample AC-C₆D₁₂-55). The detailed description of the sample preparation, their quantitative characterization, and solid-state NMR measurements are given in the Supporting Information. The choice of the adsorbents was dictated by their similar molecular sizes, albeit different electronic features, and also by the fact that the dynamics of benzene on the surface of selected porous materials is well established. ^{38–44}

■ RESULTS AND DISCUSSION

The AC sample showed an intense sharp EPR signal at a field of 3348 G and a g-factor of $2.0021^{31,32}$ (Figure S1), proving the presence of unpaired electrons. Therefore, a single pulse sequence with high-power decoupling was applied first for measuring a 13 C solid-state NMR spectrum of a static sample. However, this leads to the appearance of 13 C background signals from standard NMR probe heads. Unfortunately, spinecho experiments could not be used to suppress the signal originating from the probe head because they also remove the signal of the benzene on the AC. Therefore, to identify the 13 C NMR resonances of the sample AC-C₆D₆-370, its static 13 C{ 1 H} NMR spectrum was recorded at 295 K (Figure 1,

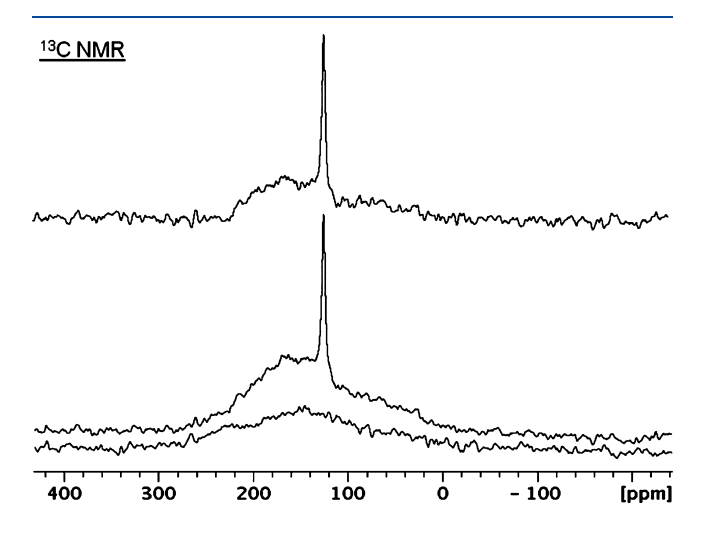


Figure 1. Static $^{13}C\{^{1}H\}$ solid-state NMR spectra recorded under identical conditions for AC-C₆D₆-370 (middle) and the empty rotor (bottom) at 295 K. The top trace shows the difference spectrum.

middle). Then, the background signal was obtained by measuring the empty rotor in the NMR probe head under identical conditions (Figure 1, bottom). Subtracting the background signal resulted in a broad signal and a narrow resonance residing on top of it (Figure 1, top). The sharp peak at $\delta(^{13}\mathrm{C})=126$ ppm belongs to the isotropically moving liquid-like benzene molecules. The very broad resonance with a shape similar to that observed for graphite stems from the AC support. Deconvolution of these signals allows the determination of their relative integrals and the benzene content in the sample. The same approach has been used to characterize AC-C₆D₆-620 and AC-C₆D₁₂-55 (Figure S2). For the latter, the corresponding static spectrum shows the isotropically moving molecules of cyclohexane- d_{12} ($\delta=23.4$ ppm).

The Hahn echo ²H NMR spectra of the static samples AC-C₆D₆-370 and AC-C₆D₆-620 were measured at temperatures between 175 and 295 K (Figure 2 and Figure S3). In accord

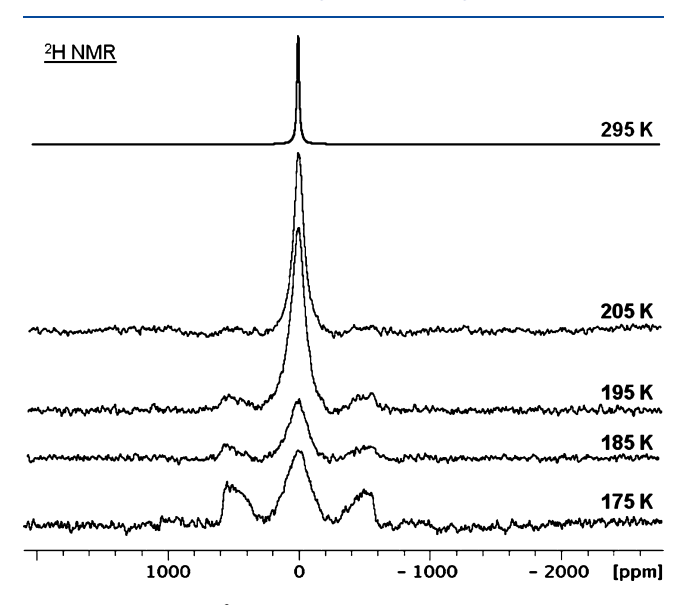
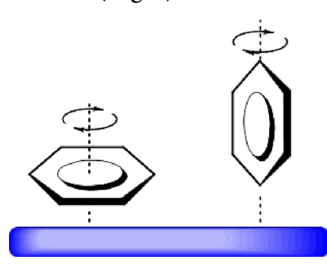


Figure 2. Hahn echo 2 H NMR spectra of the static sample AC-C₆D₆-370 at the indicated temperatures.

with ^{13}C NMR, at 295 K, only the 2H resonance with Lorentzian line shape is observed that is characteristic for the isotropically moving benzene molecules of $AC\text{-}C_6D_6\text{-}370$ (Figure 2, top). Upon cooling, the signal broadens but remains liquid-like even at 175 K, which is a temperature significantly lower than the benzene melting point (278 K). This effect is caused by the well-known melting point depression that depends on pore sizes. 42

As Figure 2 shows, the isotropic resonance experiences spectral evolution and at 175 K, the quadrupolar Pake pattern $^{42-44}$ manifests while the broadened central component is still present. The Pake pattern obviously belongs to adsorbed benzene molecules that are no longer translationally mobile but located at a specific site on the AC surface. These "stationary" molecules are depicted in Scheme 1 (left). The Pake patterns are identical for AC-C₆D₆-370 and AC-C₆D₆-620 (Figure S4) and can be simulated with a quadrupolar coupling constant ($C_{\rm Q}$) of 92 \pm 3 kHz. This value is characteristic for Pake patterns of C₆D₆ molecules on surfaces of other porous systems, $^{37-41}$ where they are oriented parallel to the surface and perform fast in-plane C₆ rotation (Scheme 1,

Scheme 1. Surface-Adsorbed Benzene Molecules Experiencing Fast In-Plane C₆ Rotation (Left) and Semibound Molecules (Right)



left). This is in accordance with the NMR data obtained for nonporous graphite²⁶ and charcoal²⁷ as support materials. The parallel orientation of the benzene ring to the surface was also suggested earlier for a graphite support based on X-ray diffraction studies.¹⁰

Recent TEM (transmission electron microscopy) experiments have demonstrated that hexagonal and pentagonal rings, as in fullerene-type structures, are present in activated carbon. ³⁰ Both five- and six-membered rings will promote π -p interactions²⁵ as a driving force for benzene adsorption.

Importantly, these π -p interactions constitute a direct mechanism that affects the ^{13}C NMR resonance of benzene molecules located on the paramagnetic **AC** surface. In fact, even at room temperature, the ^{13}C NMR resonance of the isotropically moving C_6D_6 molecules exhibits a ^{13}C T_1 relaxation time of 0.63 s, which is unusually short even for liquids. The $^{13}C\{^1H\}$ static NMR spectra of **AC-C**₆**D**₆-370 were recorded under the same conditions at 295 and 175 K (Figure 3). In both spectra, the probe head background is

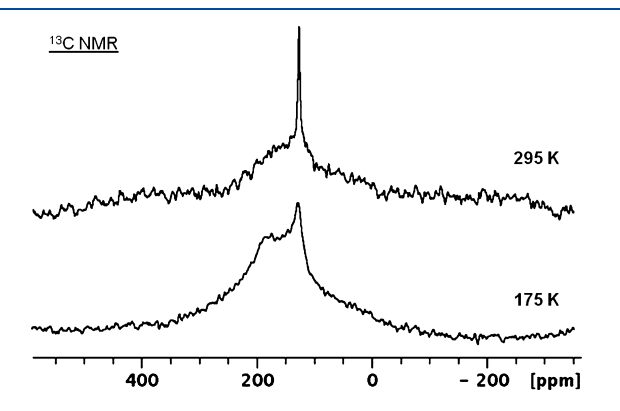


Figure 3. $^{13}C\{^{1}H\}$ NMR spectra of a static sample of AC-C₆D₆-370 at 295 K (top) and 175 K (bottom).

obviously present. Therefore, comparison of the spectra in Figures 1 and 2 allows to identify a broad line with a maximum at about 160-180 ppm (instead of the axially symmetric pattern observed in ref 27, which obviously belongs to stationary molecules (Scheme 1, left). We believe that this dramatic broadening, caused by 13 C nucleus/electron dipolar coupling of benzene with the paramagnetic pore surface of AC, strongly proves their π -p interactions.

The chemical exchange between stationary and isotropically moving C_6D_6 molecules is slow on the deuterium NMR timescale in the temperature range from 175 to 295 K (Figure 2 and Figure S3). Therefore, relative populations of these molecular states can easily be determined under these conditions. The mole fractions of stationary (P_{stat}) and

isotropically moving, mobile benzene molecules ($P_{\rm mob}$), determined for AC-C₆D₆-370 at different temperatures, are given in Table 1.

Table 1. Temperature Dependence of Stationary (P_{stat}) and Mobile (P_{mob}) Mole Fractions of AC-C₆D₆-370 and the Corresponding Equilibrium Constants $K_{\text{eq}}^{\ a}$

T (K)	$P_{ m stat}$	$P_{ m mob}$	$K_{ m eq}$
205	0.12	0.88	0.14
195	0.18	0.81	0.23
185	0.36	0.64	0.57
175	0.46	0.54	0.86

 a The averaged values obtained by two independent experiments are reported.

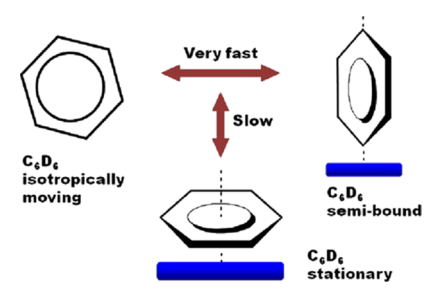
The fraction P_{stat} grows upon cooling and results in a straight line when $ln(K_{eq})$ is plotted versus 1/T. This line corresponds to a free enthalpy (ΔH^0) value of -4.6 ± 0.3 kcal/mol, which characterizes the benzene-surface interactions. This value has been determined for the first time by NMR spectroscopy. It should be noted that the absolute value, accepted as the adsorption enthalpy of benzene on AC, is close to the lowest enthalpy (-4.97 kcal/mol) reported for benzene adsorption on activated carbons, ranging from -4.97 to -10.7 kcal/mol in thermochemical experiments.²² We assume that the ΔH^0 value determined here by NMR characterizes the surface π -p interactions of benzene with the AC surface better. It is furthermore remarkable that the obtained enthalpy is larger than the fusion enthalpy of benzene (2.4 kcal/mol) and closer to the range of values (2.87 to 4.73 kcal/mol) obtained by MP2 calculations for π – π interactions in benzene dimers with parallel-displaced and sandwich orientations.⁴⁵

In contrast to benzene that displays surface π –p interactions, cyclohexane- d_{12} in the sample AC-C₆D₁₂-55 does not show a stationary state in the ²H NMR spectra (Figure S5). Even at the lowest temperatures, only one signal with Lorentzian line shape is observed. In accordance with this result, no ¹³C NMR resonance of stationary cyclohexane is detected at 175 K (Figure S6). The resonance observed is not even broadened by the paramagnetic nature of the AC surface. It is obvious that the cyclohexane/AC surface energy is significantly lower.

One spectral effect observed in this study remains to be clarified. The central component in the ²H NMR spectra of AC-C₆D₆-370 and AC-C₆D₆-620 broadens substantially upon cooling (Figure 2, Figure S3, and Table S1) although the chemical exchange between stationary and mobile C₆D₆ molecules is slow on the ²H NMR timescale. In analogy, a broadening effect is also observed for the ²H resonance of cyclohexane in AC-C₆D₁₂-55 (Table S1). However, the broadening is much less pronounced, as the half-width of the central component ($\Delta \nu$) equals nearly 12.6 kHz in the case of $AC-C_6D_6-370$ at 175 K, while it is only 4.7 kHz for $AC-C_6D_{12}$ -55. Since the large value of 12.6 kHz cannot be explained by the ²H relaxation, the broadening of the central component might be the consequence of a fast chemical exchange between the isotropically moving C₆D₆ molecules and an additional mode of mobility, called here a "semibound" state (Scheme 2). In this case, the magnitude of $\Delta \nu$ will depend on an exchange rate constant k_{exch} .

In general, the nature of the semibound state is unclear. Nevertheless, the experiments show that this state actually has

Scheme 2. Exchange between Isotropically Moving, Semibound, and Stationary C₆D₆ Molecules Adsorbed on **Activated Carbon**



to exist as an intermediate in the exchange between isotropically moving and stationary molecules. The most likely scenario for this intermediate state of adsorbed benzene is represented by the molecules being oriented perpendicular to the surface and rotating around the C₁···C₄ axis, as shown in Scheme 1.29 In fact, according to calculations performed by different methods, sandwich and T-complexes in benzene dimers are energetically almost identical, with a slight preference of T-complexes. 47-50 Regarding 2H NMR, this fast rotation will not affect the static C_Q of 180 kHz for the C-D bonds lying on this axis, while the other C-D bond vectors, defining an angle of 60° with the rotational axis, will reduce $C_{\rm O}$ to 23 kHz via eq 1.

$$\Delta \nu \text{(splitting)} = \frac{3}{4}180 \text{ (kHz)} (3 \cos^2 \theta - 1)/2$$
 (1)

Here, $\Delta \nu$ stands for the quadrupolar splitting ($\Delta \nu = 3/4C_{\rm Q}$). 51,52

To support this assumption, the ²H NMR spectrum of the static sample AC-C₆D₆-620, containing the largest amount of C₆D₆, was recorded at 175 K with 3000 scans. Figure 4 (bottom) shows this spectrum after careful phase and baseline corrections have been performed. The signal pattern can accurately be simulated with four subspectra (Figure 4, top) in agreement with the proposed surface-binding models for C₆D₆ (Schemes 1 and 2). Hereby, the pattern with a C_Q of 93 kHz is not broadened, while the other signals require large linewidths of about 6 kHz because of the chemical exchange described above (Scheme 2). In the limits of this exchange, the decrease in the linewidth of the central component in the ²H NMR spectra of AC-C₆D₆-370 when heating the sample from 193 to 253 K is caused by the acceleration of the exchange between the semibound and isotropically moving benzene states (Scheme 2). The exchange has been approximated by a three-center exchange model, where the frequency distance of the outer peaks was taken as 15 kHz (the distance between two main singularities of the pattern with a CO of 20 kHz) and the central resonance belongs to the isotropically moving benzene molecules. The three-center fitting procedures lead to the rate constants k_{exch} summarized in Table 2. The corresponding temperature dependence in the coordinates $ln(k_{exch})$ versus 1/ T (Figure S7) results in an activation energy, E_{act} , of 3.1 \pm 0.3 kcal/mol and enthalpy and entropy changes, ΔH^{\ddagger} and ΔS^{\ddagger} , of 2.7 ± 0.3 kcal/mol and -21 e.u., respectively. We believe that the relatively large negative magnitude of ΔS^{\ddagger} is caused by the approximated character of the line shape analysis.

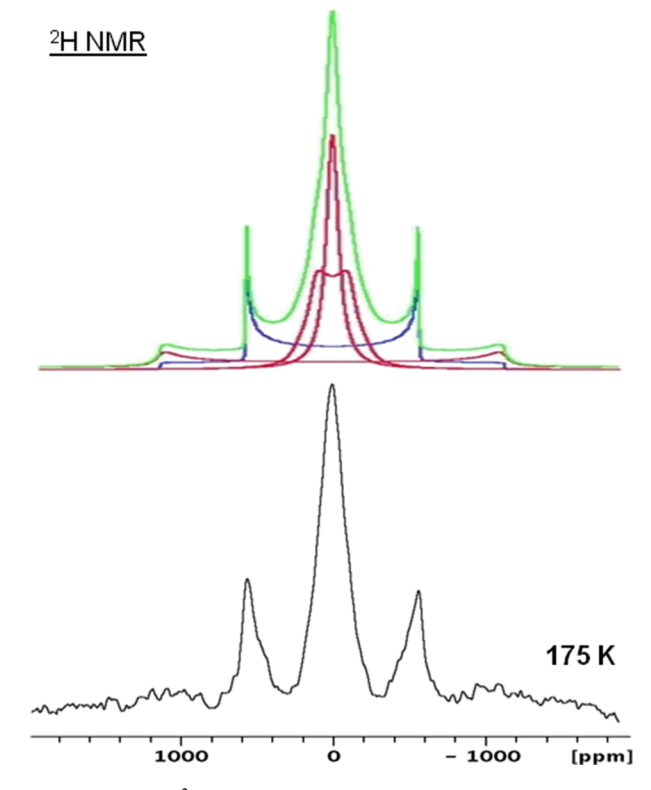


Figure 4. Static ²H NMR spectrum of AC-C₆D₆-620 at 175 K (bottom) and simulation of this spectrum using four different spectral patterns (top), $C_{\rm O}(1)$ = 187.0 kHz with η = 0.15 (two deuterium atoms located on the rotation axis at $\theta = 0^{\circ}$), $C_{\rm O}(2) = 20$ kHz with η = 0.15 (four deuterium atoms at θ = 60°), $C_{\rm O}(3)$ = 95 kHz with η = 0.05 (C_6 rotation), and $C_Q(4) = 0$ (isotropic motions).

Table 2. Rate Constants $k_{\rm exch}$ Obtained for the Chemical Exchange between the Semibound and Free Benzene Molecules (Scheme 2)

T (K)	$k_{\rm exch} \ (10^3 \cdot \mathrm{s}^{-1})$
193	68
203	89
213	120
233	230
253	480

CONCLUSIONS

In summary, molecular motions of benzene- d_6 , surfaceadsorbed within the pores of AC, have been characterized for the first time by solid-state NMR. Isotropically moving and stationary molecules, as well as molecules in intermediate states in exchange with isotropically moving molecules, have been identified. The stationary molecules, stabilized by π -p interactions with the AC surface, experience fast in-plane C₆ rotations. Benzene molecules in semibound states, similar to Tcomplexes in benzene dimers, rotate perpendicular to the surface, as depicted in Scheme 1. The adsorption enthalpy $-\Delta H^0$ for benzene on the pore surface of AC has been determined as 4.6 ± 0.3 kcal/mol. This value is larger than the binding π - π interactions in benzene dimers calculated for the gas phase,44-47 but it is smaller than the adsorption enthalpy found for the horizontally oriented molecules of ferrocene on the pore surface of AC.²⁷ Finally, the exchange between semibound and isotropically moving benzene molecules is fast, requiring only a low activation energy.

ASSOCIATED CONTENT

Supporting Information

The Supporting Information is available free of charge at https://pubs.acs.org/doi/10.1021/acs.jpcc.0c06225.

Detailed description of materials and methods used for solid-state NMR spectroscopy and additional spectra and data (PDF)

AUTHOR INFORMATION

Corresponding Authors

Vladimir I. Bakhmutov — Department of Chemistry, Texas A&M University, College Station, Texas 77843, United States; orcid.org/0000-0002-5011-0385; Email: bakhmoutov@chem.tamu.edu

Janet Blümel — Department of Chemistry, Texas A&M University, College Station, Texas 77843, United States; orcid.org/0000-0002-6557-3518; Email: bluemel@tamu.edu

Author

Jordon W. Benzie – Department of Chemistry, Texas A&M University, College Station, Texas 77843, United States

Complete contact information is available at: https://pubs.acs.org/10.1021/acs.jpcc.0c06225

Notes

The authors declare no competing financial interest.

ACKNOWLEDGMENTS

This work was supported by the National Science Foundation (CHE-1900100) and by Texas A&M University. We thank Dr. Patrick J. Hubbard for improving some of the figures.

REFERENCES

- (1) Marsh, H.; Rodriguez-Reinoso, F. Activated Carbon; Elsevier: Oxford, 2006.
- (2) Bubanale, S.; Shivashankar, M. History, Method of Production, Structure and Applications of Activated Carbon. *Int. J. Eng. Res. Technol.* **2017**, *6*, 495–497.
- (3) Turov, V. V.; Leboda, R. ¹H NMR Chemical shifts of adsorbed molecules on the carbon surface. *Adsorpt. Sci. Technol.* **1998**, *16*, 837–855.
- (4) Harris, R. K.; Thompson, T. V.; Forshaw, P.; Foley, N.; Thomas, K. M.; Norman, P. R.; Pottage, C. A magic-angle spinning NMR study into the adsorption of deuterated water by activated carbon. *Carbon* **1996**, *34*, 1275–1279.
- (5) Cosnier, F.; Celzard, A.; Furdin, G.; Bégin, D.; Marêché, J. F.; Barrès, O. Hydrophobisation of active carbon surface and effect on the adsorption of water. *Carbon* **2005**, *43*, 2554–2563.
- (6) Kim, P.; Agnihotri, S. Application of water—activated carbon isotherm models to water adsorption isotherms of single-walled carbon nanotubes. *J. Colloid Interface Sci.* **2008**, 325, 64–73.
- (7) Sliwinska-Bartkowiak, M.; Jazdzewska, M.; Huang, L. L.; Gubbins, K. E. Melting behavior of water in cylindrical pores: carbon nanotubes and silica glasses. *Phys. Chem. Chem. Phys.* **2008**, *10*, 4909–4919.
- (8) Cabrera-Sanfelix, P.; Darling, G. R. Dissociative Adsorption of Water at Vacancy Defects in Graphite. *J. Phys. Chem. C* **2007**, 111, 18258–18263.
- (9) Collignon, B.; Hoang, P. N. M.; Picaud, S.; Rayez, J. C. Ab initio study of the water adsorption on hydroxylated graphite surfaces. *Chem. Phys. Lett.* **2005**, *406*, 430–435.
- (10) Ueno, Y.; Muramatsu, Y.; Grush, M. M.; Perera, R. C. C. Configurations of Benzene and Pyridine Molecules Adsorbed on

- Graphitic Surface of Microporous Carbon. J. Phys. Chem. B 2000, 104, 7154–7162.
- (11) Kowalczyk, P.; Ustinov, E. A.; Terzyk, A. P.; Gauden, P. A.; Kaneko, K.; Rychlicki, G. Description of benzene adsorption in slit-like pores. Theoretical foundations of the improved Horvath–Kawazoe method. *Carbon* **2004**, *42*, 851–864.
- (12) Ueno, Y.; Muramatsu, Y. Direct observation of benzene and pyridine molecules adsorbed in microporous carbon using synchrotron-radiation-excited soft X-ray emission spectroscopy. *Carbon* **2000**, 38, 1939–1942.
- (13) Birkett, G. R.; Do, D. D. Simulation study of water adsorption on carbon black: the effect of graphite water interaction strength. *J. Phys. Chem. C* **2007**, *111*, 5735–5742.
- (14) Smith, M. R., Jr.; Hedges, S. W.; LaCount, R.; Kern, D.; Shah, N.; Huffman, G. P.; Bockrath, B. Selective oxidation of single-walled carbon nanotubes using carbon dioxide. *Carbon* **2003**, *41*, 1221–1230.
- (15) Marosfői, B. B.; Szabó, A.; Marosi, G.; Tabuani, D.; Camino, G.; Pagliari, S. Thermal and spectroscopic characterization of polypropylene-carbon nanotube composites. *J. Therm. Anal. Calorim.* **2006**, *86*, 669–673.
- (16) Maniwa, Y.; Sato, M.; Kume, K.; Kozlov, M. E.; Tokumoto, M. Comparative NMR study of new carbon forms. *Carbon* **1996**, *34*, 1287–1291.
- (17) Darmstadt, H.; Roy, C.; Kaliaguine, S.; Xu, G.; Auger, M.; Tuel, A.; Ramaswamy, V. Solid state ¹³C-NMR spectroscopy and XRD studies of commercial and pyrolytic carbon blacks. *Carbon* **2000**, 38, 1279–1287.
- (18) Freitas, J. C. C.; Emmerich, F. G.; Cernicchiaro, G. R. C.; Sampaio, L. C.; Bonagamba, T. J. Magnetic Susceptibility Effects on ¹³C MAS NMR Spectra of Carbon Materials and Graphite. *Solid-State Nucl. Magn. Reson.* **2001**, *20*, 61–73.
- (19) Cluff, K. J.; Blümel, J. Adsorption of ferrocene on carbon nanotubes, graphene, and activated carbon. *Organometallics* **2016**, *35*, 3939–3948.
- (20) Wibowo, N.; Setyadhi, L.; Wibowo, D.; Setiawan, J.; Ismadji, S. Adsorption of Benzene and Toluene from Aqueous Solutions onto Activated Carbon and its Acid and Heat Treated Forms: Influence of Surface Chemistry on Adsorption. *J. Hazard. Mater.* **2007**, *146*, 237–242.
- (21) Dubinin, M. M.; Polyakov, N. S.; Kataeva, L. I. Basic Properties of Equations for Physical Vapor Absorption in Micropores of Carbon Adsorbents Assuming a Normal Micropore Distribution. *Carbon* **1991**, *29*, 481–488.
- (22) Chiang, H. L.; Huang, C. P.; Chiang, P. C. The Adsorption of Benzene and Methylethylketone onto Activated Carbon: Thermodynamic aspects. *Chemosphere* **2002**, *46*, 143–152.
- (23) Hindarso, H.; Ismadji, S.; Wicaksana, F.; Mudjijati; Indraswati, N. Adsorption of Benzene and Toluene from Aqueous Solution onto Granular Activated Carbon. *J. Chem. Eng. Data* **2001**, *46*, 788–791.
- (24) Basso, M. C.; Cukierman, A. L. Arundo Donax-Based Activated Carbons for Aqueous-Phase Adsorption of Volatile Organic Compounds. *Ind. Eng. Chem. Res.* **2005**, *44*, 2091–2100.
- (25) Xu, Y.; Watermann, T.; Limbach, H.-H.; Gutmann, T.; Sebastiani, D.; Buntkowsky, G. Water and small organic molecules as probes for geometric confinement in well-ordered mesoporous carbon materials. *Phys. Chem. Chem. Phys.* **2014**, *16*, 9327–9336.
- (26) Voss, V.; Boddenberg, B. Anisotropic reorientation dynamics of benzene molecules adsorbed on graphite, alumina, and zeolite Y. *Surf. Sci.* **1993**, 298, 241–250.
- (27) Kaplan, S.; Resing, H. A.; Waugh, J. S. ¹³C NMR chemical shift anisotropy for benzene adsorbed on charcoal and silica gel. *J. Chem. Phys.* **1973**, *59*, 5681–5687.
- (28) Hubbard, P. J.; Benzie, J. W.; Bakhmutov, V. I.; Blümel, J. Ferrocene Adsorbed on Silica and Activated Carbon Surfaces: A Solid-State NMR Study of Molecular Dynamics and Surface Interactions. *Organometallics* **2020**, *39*, 1080–1091.

- (29) Klomkliang, N.; Do, D. D.; Nicholson, D. Affinity and Packing of Benzene, Toluene, and p-Xylene Adsorption on a Graphitic Surface and in Pores. *Ind. Eng. Chem. Res.* **2012**, *51*, 5320–5329.
- (30) Harris, P. J. F.; Liu, Z.; Suenaga, K. Imaging the atomic structure of activated carbon. *J. Phys. Condens. Matter* **2008**, 20, 362201–362206.
- (31) Kempiński, M.; Śliwińska-Bartkowiak, M.; Kempiński, W. Molecules in the porous system of activated carbon fibers: spin population control. *Rev. Adv. Mater. Sci.* **2007**, *14*, 163–166.
- (32) Więckowski, A. B.; Najder-Kozdrowska, L.; Rechnia, P.; Malaika, A.; Krzyżyńska, B.; Kozłowski, M. EPR Characteristics of activated carbon for hydrogen production by the thermo-catalytic decomposition of methane. *Acta Phys. Pol. A* **2016**, *130*, 701–704.
- (33) Schnellbach, M.; Köhler, F. H.; Blümel, J. The Union Carbide Catalyst (Cp₂Cr + SiO₂), Studied by Solid-State NMR. *J. Organomet. Chem.* **1996**, 520, 227–230.
- (34) Cluff, K. J.; Blümel, J. Adsorption of Metallocenes on Silica. *Chem. Eur. J.* **2016**, 22, 16562–16575.
- (35) Bartuś, K.; Bródka, A. Methane behavior in carbon nanotube as a function of pore filling and temperature studied by molecular dynamics simulations. *J. Phys. Chem. C* **2017**, *121*, 4066–4073.
- (36) Bartuś, K.; Bródka, A. Temperature study of structure and dynamics of methane in carbon nanotubes. *J. Phys. Chem. C* **2014**, *118*, 12010–12016.
- (37) Sun, J.; Hippo, E. J.; Marsh, H.; O'Brien, W. S.; Crelling, J. C. Activated carbon produced from an Illinois basin coal. *Carbon* 1997, 35, 341–352.
- (38) Gonzalez, J.; Devi, R. N.; Tunstall, D. P.; Cox, P. A.; Wright, P. A. Deuterium NMR studies of framework and guest mobility in the metal-organic framework compound MOF-5, Zn₄O-(O₂CC₆H₄CO₂)₃. Microporous Mesoporous Mater. **2005**, 84, 97–104.
- (39) Gedat, E.; Schreiber, A.; Albrecht, J.; Emmler, T.; Shenderovich, I.; Findenegg, G. H.; Limbach, H.-H.; Buntkowsky, G. ²H-Solid-State NMR Study of Benzene-d₆ Confined in Mesoporous Silica SBA-1. *J. Phys. Chem. B* **2002**, *106*, 1977–1984.
- (40) Gonzalez, J.; Devi, R. N.; Wright, P. A.; Tunstall, D. P.; Cox, P. A. Motion of aromatic hydrocarbons in the microporous aluminum methylphosphonates AlMePO- α and AlMePO- β . *J. Phys. Chem. B* **2005**, *109*, 21700–21709.
- (41) Xu, J.; Sinelnikov, R.; Huang, Y. Capturing guest dynamics in metal—organic framework CPO-27-M (M = Mg, Zn) by ²H solid-state NMR Spectroscopy. *Langmuir* **2016**, *32*, 5468–5479.
- (42) Buntkowsky, G.; Breitzke, H.; Adamczyk, A.; Roelofs, F.; Emmler, T.; Gedat, E.; Grunberg, B.; Xu, Y.; Limbach, H.-H.; Shenderovich, I. ²H-Solid-state NMR study of benzene-d₆ confined in mesoporous silica SBA-15. *Phys. Chem. Chem. Phys.* **2007**, *9*, 4843–4853
- (43) Xiong, J.; Maciel, G. E. Deuterium NMR studies of local motions of benzene adsorbed on Ca-montmorillonite. *J. Phys. Chem. B* **1999**, *103*, 5543–5549.
- (44) Aliev, A. E.; Harris, D. M.; Mahdyarfar, A. Dynamics of benzene and pyridine guest molecules in their TOT inclusion compounds: solid-state ²H NMR studies. *J. Chem. Soc., Faraday Trans.* 1995, 91, 2017–2026.
- (45) Sinnokrot, M. O.; Sherrill, C. D. High-accuracy quantum mechanical studies of π π interactions in benzene dimers. *J. Phys. Chem. A* **2006**, *110*, 10656–10668.
- (46) Harris, R. K. Nuclear magnetic resonance, a physicochemical view; Pitman Publishing Inc.: Toronto 1983, p. 119–122.
- (47) Sinnokrot, M. O.; Valeev, E. F.; Sherrill, C. D. Estimates of the ab initio limit for π - π interactions: the benzene dimer. *J. Am. Chem. Soc.* **2002**, 124, 10887–10893.
- (48) Chipot, C.; Jaffe, R.; Maigret, B.; Pearlman, D. A.; Kollman, P. A. Benzene Dimer: A Good Model for for π π Interactions in Proteins? A Comparison between the Benzene and the Toluene Dimers in the Gas Phase and in an Aqueous Solution. *J. Am. Chem. Soc.* 1996, 118, 11217–11224.
- (49) Tummanapelli, A. K.; Vasudevana, S. Communication: Benzene dimer—The free energy landscape. *J. Chem. Phys.* **2013**, *139*, 201102.

- (50) Park, Y. C.; Lee, J. S. Accurate ab initio binding energies of the benzene dimer. *J. Phys. Chem. A* **2006**, *110*, 5091–5095.
- (51) Gielen, M.; Willem, R.; Wrackmeyer, B. Unusual Structures and Physical Properties in Organometallic Chemistry; Wiley: West Sussex, 2002; p.152.
- (52) Fyfe, C. A. Solid-State NMR for Chemists; C.F.C. Press: Guelph, Canada, 1983.